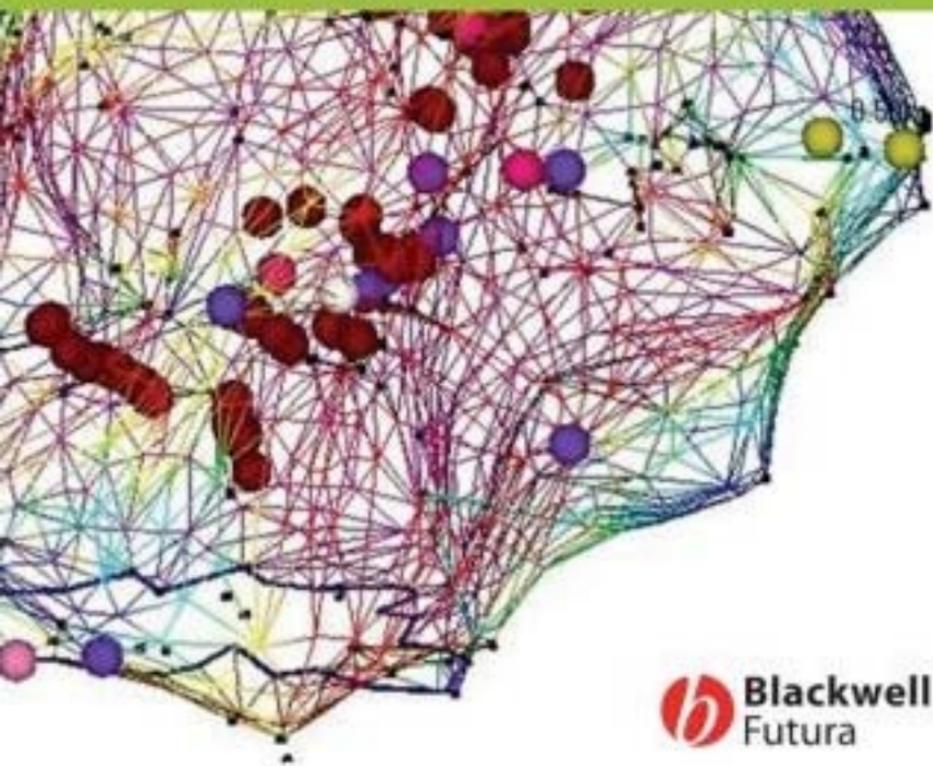# Ventricular Arrhythmias and Sudden Cardiac Death

Mechanism, Ablation, and Defibrillation

Edited by

Paul Wang, Henry Hsia, Amin Al-Ahmad, Paul Zei

Ventricular Arrhythmias and Sudden Cardiac Death

Ventricular Arrhythmias and Sudden Cardiac Death

EDITED BY

Paul J. Wang, MD

Cardiac Arrhythmia Service
Stanford University Medical Center
Stanford, CA
USA

Amin Al-Ahmad, MD

Cardiac Arrhythmia Service
Stanford University Medical Center
Stanford, CA
USA

Henry H. Hsia, MD

Cardiac Arrhythmia Service
Stanford University Medical Center
Stanford, CA
USA

Paul C. Zei, MD, PhD

Cardiac Arrhythmia Service
Stanford University Medical Center
Stanford, CA
USA

Blackwell Futura

Contents

Contributors

Amin Al-Ahmad, MD
Cardiac Arrhythmia Service
Stanford University Medical Center
Stanford, CA
USA

Charles Antzelevitch, PhD
Masonic Medical Research Laboratory
Utica, NY
USA

Nitish Badhwar, MBBS, FACC
Section of Cardiac Electrophysiology
UCSF, Division of Cardiology
University of California
San Francisco, CA
USA

Marci S. Bailey, RN
Research Coordinator
Washington University School of Medicine
St. Louis, MO
USA

J. Thomas Bigger, MD
Columbia University College of Physicians and Surgeons
New York, NY
USA

J. David Burkhardt
Cardiac Pacing and Electrophysiology
Department of Cardiovascular Medicine
Cleveland Clinic Foundation
Cleveland, OH
USA

Hugh Calkins, MD
Professor of Medicine
Director of the Arrhythmia Service
Director of the Electrophysiology Laboratory
Director of the Johns Hopkins ARVD
    Program Johns Hopkins Medical Institutions
Baltimore, MD
USA

David J. Callans, MD
University of Pennsylvania Health System
Philadelphia, PA
USA

Lan S. Chen, MD
The Department of Neurology
Indiana University School of Medicine
Indianapolis, Indiana
USA

Peng-Sheng Chen, MD
The Krannert Institute of Cardiology
Division of Cardiology
Department of Medicine
Indiana University School of Medicine
Indianapolis, IN
USA

Ralph J. Damiano, Jr. MD
Chief of Cardiothoracic Surgery
John Shoenberg Professor of Surgery
Washington University School of Medicine
St. Louis, MO
USA

Jacques MT de Bakker, PhD
Head, Department of Experimental Cardiology Academic
    Medical Center; Amsterdam, The Netherlands

The Center of Heart Failure Research, Department of
    Experimental Cardiology, Academic Medical Center,
    Amsterdam, The Netherlands
The Heart Lung Center, University Medical Center Utrecht,
    The Netherlands
The Department of Medical Physiology, University Medical
    Center Utrecht, The Netherlands
The Interuniversity Cardiology Institute of the Netherlands,
    Utrecht
The Netherlands

Derek J. Dosdall, PhD
University of Alabama at Birmingham
Department of Biomedical Engineering
Birmingham, AL
USA

N.A. Mark Estes III, MD
Professor of Medicine
Director, Cardiac Arrhythmia Center
Tufts University School of Medicine
Boston, MA
USA

Ilan Goldenberg, MD
The Cardiology Division
Department of Medicine
University of Rochester Medical Center
Rochester, NY
USA

Jeffrey J. Goldberger, MD
The Division of Cardiology
Department of Medicine
Feinberg School of Medicine
Northwestern University
Chicago, IL
USA

Anurag Gupta, MD
Stanford University Medical Center
Stanford, CA
USA

Mark C. Haigney, MD
Uniformed Services University
Bethesda, MD
USA

Munther Homoud, MD
Tufts-New England Medical Center
Boston, MA
USA

Henry H. Hsia, MD
Cardiac Arrhythmia Service
Stanford University Medical Center
Stanford, CA
USA

Jian Huang, MD, PhD
University of Alabama at Birmingham
Departments of Medicine
Birmingham, AL
USA

Mathew D. Hutchinson, MD
University of Pennsylvania Health System
Philadelphia, PA
USA

Raymond E. Ideker, MD, PhD
University of Alabama at Birmingham
Departments of Physiology and Biomedical
   Engineering Medicine
Birmingham, AL
USA

Rahul Jain, MD
Division of Cardiology
The Johns Hopkins University School of
   Medicine
MD
USA

Robert E. Kleiger, MD
Washington University School of Medicine
St. Louis, MO
USA

Keane K. Lee, MD
Stanford University Medical Center
Stanford, CA
USA

Mark S. Link, MD
Tufts-New England Medical Center
Boston, MA
USA

Kevin J. Makati, MD
Tufts-New England Medical Center
Boston, MA
USA

Barry J. Maron, MD
Hypertrophic Cardiomyopathy Center
Minneapolis Heart Institute Foundation
MN
USA

Pirooz S. Mofrad, MD
Stanford University Medical Center
Standford, CA
USA

Robert J. Moraca, MD
Fellow in Cardiothoracic Surgery
Washington University School of Medicine
St. Louis, MO
USA

Arthur J. Moss, MD
Professor of Medicine (Cardiology)
Director, Heart Research Follow-Up
    Program
University of Rochester Medical Center
Rochester, NY
USA

Robert J. Myerburg, MD, FACC
Professor of Medicine and Physiology
Chief, Division of Cardiology
University of Miami
Miami, FL
USA

Andrea Natale, MD
Section Head, Electrophysiology and Pacing
Director of the Electrophysiology Laboratories
The Cleveland Clinic Foundation
Cleveland, OH
USA

Jeffrey Olgin, MD
Section of Cardiac Electrophysiology
Division of Cardiology
University of California, San Francisco
San Francisco, CA
USA

Marco Perez, MD
Stanford University
Stanford, CA
USA

Karen P. Phillips, MB, BS (Hons), FRACP
Clinical Cardiac Electrophysiology Fellow
Department of Cardiovascular Medicine
Cleveland Clinic Foundation
Cleveland, OH
USA

Walid I. Saliba, MD
Director, Electrophysiology Laboratories
Section of Cardiac Pacing and Electrophysiology
Department of Cardiovascular Medicine
Cleveland Clinic Foundation
Cleveland, OH
USA

Mauricio Scanavacca, MD
Heart Institute
University of Sao Paulo Medical School
Sao Paulo
Brasil

Melvin M. Scheinman, MD, FACC
Section of Cardiac Electrophysiology
University of California, San Francisco
San Francisco, CA
USA

Robert A. Schweikert, MD
Director, EP Clinical Operations
Section of Cardiac Electrophysiology and Pacing
Department of Cardiovascular Medicine
Cleveland Clinic Foundation
Cleveland, OH
USA

Kyoko Soejima, MD
Assistant Professor
Division of Cardiology
Keio University
Tokyo
Japan

Eduardo Sosa, MD
Heart Institute
University of Sao Paulo Medical School
Sao Paulo
Brazil

Moshe S, Swissa, MD
Division of Cardiology
Department of Medicine
Kaplan Medical Center, Rehovot
The Hebrew University, Jerusalem
Israel

William G. Stevenson, MD
Director, Clinical, Cardiac Electrophysiology, Program
Cardiovascular Division
Brigham and Women's Hospital
Boston, MA
USA

Usha Tedrow, MD
Associate Director, Clinical Cardiac,
    Electrophysiology, Program
Cardiovascular Division
Brigham and Women's Hospital
Boston, MA
USA

Zian H. Tseng, MD
Section of Cardiac Electrophysiology
Division of Cardiology
University of California, San Francisco
San Francisco, CA
USA

George F. Van Hare, MD
Professor of Pediatrics, Clinical Professor of Pediatrics;
    and Director, Pediatric Arrhythmia Center
Stanford University School of Medicine and UCSF
Palo Alto, CA
USa

Harold VM van Rijen
The Department of Medical Physiology
University Medical Center Utrecht
The Netherlands

Paul J. Wang, MD
Stanford University Medical Center
Stanford, CA
USA

Oussama Wazni, MD
Associate Director
Cleveland Clinic Center for Cardiovascular Research
Cleveland Clinic
Cleveland, OH
USA

Jonathan Weinstock, MD
Tufts-New England Medical Center
Boston, MA
USA

Bruce L. Wilkoff, MD
Professor of Medicine and Director, Cardiac Pacing and
Tachyarrhythmia Devices
Cleveland Clinic Foundation
Cleveland, OH
USA

Wojciech Zareba, MD, PhD
The Cardiology Division, Department of Medicine
University of Rochester Medical Center
Rochester, NY
USA

Paul C. Zei, MD, PhD
Cardiac Arrhythmia Service
Stanford University Medical Center
Stanford, CA
USA

Foreword

When, 40 years ago, intracardiac stimulation and activation studies were started for the analysis of cardiac arrhythmias, nobody could have predicted the advances that were going to be made in the years thereafter in our understanding and management of ventricular arrhythmias and sudden death.

Since then an enormous amount of information has become available, leading to our current understanding of mechanisms, etiology, epidemiology, risk stratification, and management of these, unfortunately too often occurring, life-threatening situations.

The best way to present that knowledge, and also the relation between those different areas, is to put it in the form of a book.

We live in a time when information spreads rapidly by way of the internet. However, tunnel vision is one of the dangers of that medium: the subspecialist, looking only for what is new in his or her specialized area, may lose sight of the complete picture with its inherent dangers.

Therefore one has to welcome this book for its coverage and time of publication. By selecting the contributors carefully, the editors have succeeded in bringing together, in one book, an excellent and complete overview of what the cardiologist should know for optimal management of the patient with a ventricular arrhythmia. Among the many in-depth presentations one will find how to select the candidate for catheter ablation, when to implant an ICD, and what measures have to be taken to reduce sudden death out of hospital.

Hein J. Wellens
Maastricht, The Netherlands
August 2007

CHAPTER 1

The role of spatial dispersion of repolarization and intramural reentry in inherited and acquired sudden cardiac death syndromes

Charles Antzelevitch

Abstract

The cellular basis for intramural reentry that develops secondary to the development of transmural dispersion of repolarization (TDR) is examined in this review. The hypothesis that amplification of spatial dispersion of repolarization underlies the development of intramural reentry and life-threatening ventricular arrhythmias associated with inherited ion channelopathies is probed. The roles of TDR in the long-QT, short-QT, and Brugada syndromes as well as catecholaminergic polymorphic ventricular tachycardia are critically examined. In the long-QT syndrome, amplification of TDR is generally secondary to preferential prolongation of the action potential duration (APD) of M cells, whereas in the Brugada syndrome, it is due to selective abbreviation of the APD of right ventricular epicardium. Preferential abbreviation of APD of either endocardium or epicardium appears to be responsible for amplification of TDR in the short-QT syndrome. The available data suggest that the long-QT, short-QT, and Brugada syndromes are pathologies with very different phenotypes and etiologies, but which share a common final pathway in causing sudden cardiac death.

Keywords:

long QT syndrome; short QT syndrome; Brugada syndrome; polymorphic ventricular tachycardia; electrophysiology

Inherited sudden cardiac death secondary to the development of life-threatening ventricular arrhythmias have been associated with a variety of ion channelopathies such as the long-QT, short-QT, and Brugada syndromes. Table 1.1 lists the genetic defects thus far identified to be associated with these primary electrical diseases. These ion channel defects have been shown to amplify spatial dispersion of repolarization, in some cases with the assistance of pharmacologic agents that further exaggerate the gain or loss of function of ion channel activity. Before examining these interactions, we will review the basis for intrinsic electrical heterogeneity within the ventricular myocardium.

Intrinsic electrical heterogeneity within the ventricular myocardium

It is now well established that ventricular myocardium is comprised of at least three electrophysiologically as well as functionally distinct cell types: epicardial, M, and endocardial cells [1,2]. These three principal ventricular myocardial cell types differ with respect to phase 1 and phase 3 repolarization characteristics. Ventricular epicardial and M,

Table 1.1 Inherited disorders caused by ion channelopathies

		Rhythm	*Inheritance*	*Locus*	*Ion channel*	*Gene*
Long-QT syndrome	(RW)	TdP	AD			
	LQT1		AD	11p15	I_{Ks}	*KCNQ1, KvLQT1*
	LQT2		AD	7q35	I_{Kr}	*KCNH2, HERG*
	LQT3		AD	3p21	I_{Na}	*SCN5A, Na$_v$1.5*
	LQT4		AD	4q25		*ANKB, ANK2*
	LQT5		AD	21q22	I_{Ks}	*KCNE1, minK*
	LQT6		AD	21q22	I_{Kr}	*KCNE2, MiRP1*
	LQT7	(Anderson–Tawil syndrome)	AD	17q23	I_{K1}	*KCNJ2, Kir 2.1*
	LQT8	(Timothy syndrome)	AD	6q8A	I_{Ca}	*CACNA1C, Ca$_v$1.2*
	LQT9		AD	3p25	I_{Na}	*CAV3, Caveolin-3*
	LQT10		AD	11q23.3	I_{Na}	*SCN4B, Na$_v$b4*
LQT syndrome (JLN)		TdP	AR	11p15	I_{Ks}	*KCNQ1, KvLQT1*
				21q22	I_{Ks}	*KCNE1, minK*
Brugada syndrome	BrS1	PVT	AD	3p21	I_{Na}	*SCN5A, Nav1.5*
	BrS2	PVT	AD	3p24	I_{Na}	*GPD1L*
	BrS3	PVT	AD	12p13.3	I_{Ca}	*CACNA1C, Ca$_v$1.2*
	BrS4	PVT	AD	10p12.33	I_{Ca}	*CACNB2b, Ca$_v$B$_{2b}$*
Short-QT syndrome	SQT1	VT/VF	AD	7q35	I_{Kr}	*KCNH2, HERG*
	SQT2		AD	11p15	I_{Ks}	*KCNQ1, KvLQT1*
	SQT3		AD	17q23.1-24.2	I_{K1}	*KCNJ2, Kir2.1*
	SQT4		AD	12p13.3	I_{Ca}	*CACNA1C, Ca$_v$1.2*
	SQT5		AD	10p12.33	I_{Ca}	*CACNB2b, Ca$_v$β2b*
Catecholaminergic VT	CVPT1	VT	AD	1q42-43		*RyR2*
	CPVT2	VT	AR	1p13-21		*CASQ2*

Abbreviations: AD, autosomal dominant; AR, autosomal recessive; JLN, Jervell and Lange-Nielsen; LQT, long QT; RW, Romano–Ward; TdP, Torsade de Pointes; VF, ventricular fibrillation; VT, ventricular tachycardia; PVT, polymorphic VT.

but not endocardial, cells generally display a prominent phase 1, due to a large 4-aminopyridine (4-AP)-sensitive transient outward current (I_{to}), giving the action potential either a spike-and-dome or a notched configuration. These regional differences in I_{to} were first suggested on the basis of action potential data [3] and subsequently demonstrated using patch clamp techniques in canine [4], feline [5], rabbit [6], rat [7], ferret [8], and human [9,10] ventricular myocytes.

The magnitude of the action potential notch and corresponding differences in I_{to} have also been shown to be different between right and left ventricular epicardium [11]. Similar interventricular differences in I_{to} have also been described for canine ventricular M cells [12]. This distinction is thought to form the basis for why the Brugada syndrome, a

channelopathy-mediated form of sudden death, is a right ventricular disease.

Wang and co-workers [13] reported a larger L-type calcium channel current (I_{Ca}) in canine endocardial versus epicardial ventricular myocytes, although other studies have failed to detect any difference in I_{Ca} among cells isolated from epicardium, M, and endocardial regions of the canine left ventricular wall [14,15]. Myocytes isolated from the epicardial region of the left ventricular wall of the rabbit show a higher density of cAMP-activated chloride current when compared to endocardial myocytes [16]. I_{to2}, initially ascribed to a K$^+$ current, is now thought to be caused primarily by the calcium-activated chloride current ($I_{Cl(Ca)}$); it is thought to also contribute to the action potential notch but it is not known whether this current

differs among the three ventricular myocardial cell types [17].

Characteristics of the M cell

Residing in the deep structures of the ventricular wall between the epicardial and endocardial layers, are M cells and transitional cells. The M cell, masonic midmyocardial Moe cell, discovered in the early 1990s, was named in memory of Gordon K Moe [2,18,19]. The hallmark of the M cell is that its action potential can prolong more than that of epicardium or endocardium in response to a slowing of rate or in response to agents that prolong APD (Figure 1.1) [1,18,20]. Histologically, M cells are similar to epicardial and endocardial cells. Electrophysiologically and pharmacologically, they appear to be a hybrid between Purkinje and ventricular cells [21]. Like Purkinje fibers, M cells show a prominent APD prolongation and develop early afterdepolarizations (EAD) in response to I_{Kr} blockers, whereas epicardium and endocardium do not. Like Purkinje fibers, M cells develop delayed afterdepolarizations (DAD) more readily in response to agents that calcium load or overload the cardiac cell. α_1 Adrenoceptor stimulation produces APD prolongation in Purkinje fibers, but abbreviation in M cells, and little or no change in endocardium and epicardium [22].

Although transitional cells are found throughout much of the wall in the canine left ventricle, M cells displaying the longest action potentials (at basic cycle lengths (BCLs) $\geq$ 2000 ms) are often localized in the deep subendocardium to midmyocardium in the anterior wall [23], deep subepicardium to midmyocardium in the lateral wall [18], and throughout the wall in the region of the right ventricular (RV) outflow tracts [2]. M cells are also present in the deep cell layers of endocardial structures, including papillary muscles, trabeculae, and the interventricular septum [24]. Unlike Purkinje fibers, M cells are not found in discrete bundles or islets [24,25] although there is evidence that they may be localized in discrete muscle layers. Cells with the characteristics of M cells have been described in the canine, guinea pig, rabbit, pig, and human ventricles [4,18,20,23–44].

Isolated myocytes dissociated from discrete layers of the left ventricular wall display APD values
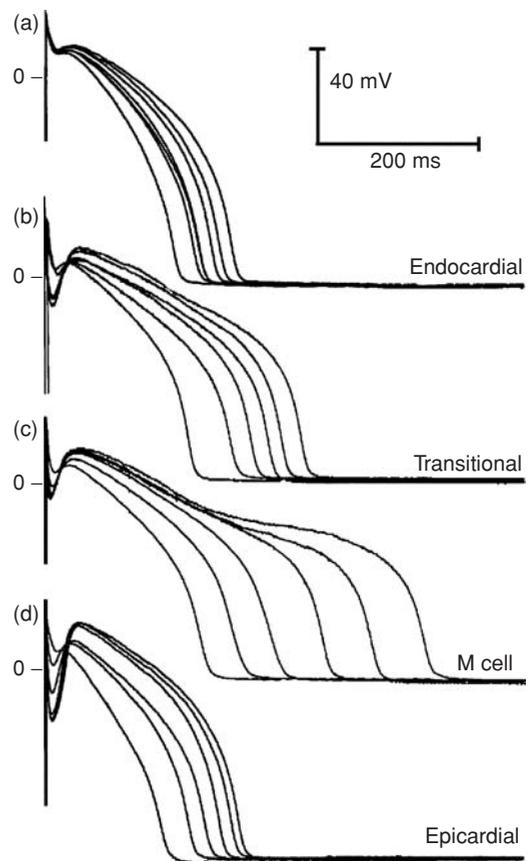
Figure 1.1 Transmembrane activity recorded from cells isolated from the epicardial, M, and endocardial regions of the canine left ventricle at basic cycle lengths (BCL) of 300–5000 milliseconds (steady-state conditions). The M and transitional cells were enzymatically dissociated from the midmyocardial region. Deceleration-induced prolongation of APD is much greater in M cells than in epicardial and endocardial cells. The spike-and-dome morphology is also more accentuated in the epicardial cell. From [4], with permission.

that differ by more than 200 milliseconds at relatively slow rates of stimulation. When the cells are in a functional syncytium that comprises the ventricular myocardium, electrotonic interactions among the different cells types lead to reduction of the APD dispersion to 25–55 milliseconds. The transmural increase in APD from epicardium to endocardium is relatively gradual, except between the epicardium and subepicardium where there is often a sharp increase in APD (Figure 1.2). This has been shown to be due to an increase in tissue
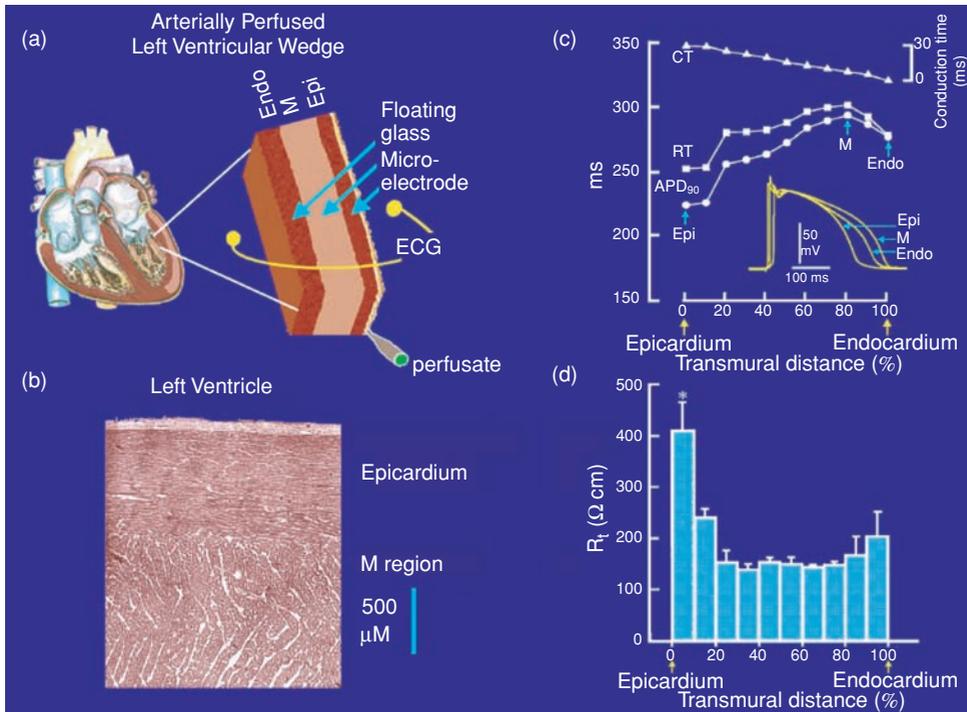
Figure 1.2 Transmural distribution of action potential duration and tissue resistivity across the ventricular wall. (a) Schematic diagram of the coronary-perfused canine LV wedge preparation. Transmembrane action potentials are recorded simultaneously from epicardial (Epi), M region (M), and endocardial (Endo) sites using three floating microelectrodes. A transmural ECG is recorded along the same transmural axis across the bath, registering the entire field of the wedge. (b) Histology of a transmural slice of the left ventricular wall near the epicardial border. The region of sharp transition of cell orientation coincides with the region of high tissue resistivity depicted in Panel (d) and the region of sharp transition of action potential duration illustrated in Panel (c). (c) Distribution of conduction time (CT), APD_{90}, and repolarization time (RT = APD_{90}+ CT) in a canine left ventricular wall wedge preparation paced at BCL of 2000 milliseconds. A sharp transition of APD_{90} is present between epicardium and subepicardium. Epi: epicardium; M: M cell; Endo: endocardium. RT: repolarization time; CT: conduction time. (d) Distribution of total tissue resistivity (R_t) across the canine left ventricular wall. Transmural distances at 0% and 100% represent epicardium and endocardium, respectively. * $P < 0.01$ compared with R_t at mid-wall. Tissue resistivity increases most dramatically between deep subepicardium and epicardium. Error bars represent SEM ($n = 5$). From [21,23], with permission.

resistivity in this region [23], which may be related to the sharp transition in cell orientation in this region as well as to reduced expression of connexin43 [45,46], which is principally responsible for intracellular communication in ventricular myocardium. Moreover, LeGrice et al. [47] have shown that the density of collagen is heterogeneously distributed across the ventricular wall. A greater density of collagen in the deep subepicardium may also contribute to the resistive barrier in this region of the wall, limiting the degree of electrotonic interaction between myocardial layers. The degree of electrotonic coupling, together with the intrinsic differences APD, contribute to TDR in the ventricular myocardium [48].

The ionic bases for these features of the M cell include the presence of a smaller slowly activating delayed rectifier current (I_{Ks}) [30], a larger late sodium current (late I_{Na}) [49], and a larger Na–Ca exchange current ($I_{Na–Ca}$) [50]. In the canine heart, the rapidly activating delayed rectifier (I_{Kr}) and the inward rectifier (I_{K1}) currents are similar in the three transmural cell types. Transmural and apico-basal differences in the density of I_{Kr} channels have been described in the ferret heart [51]. I_{Kr} message and channel protein are much larger in

the ferret epicardium. I_{Ks} is larger in M cells isolated from the right versus left ventricles of the dog [12]. These ionic distinctions sensitize the M cells to a variety of pharmacological agents. Agents that block the rapidly activating delayed rectifier current (I_{Kr}), I_{Ks}, or that increase calcium channel current (I_{Ca}) or late I_{Na}, generally produce a much greater prolongation of the APD of the M cell than of epicardial or endocardial cells leading to amplification of TDR.

Amplification of transmural heterogeneities normally present in the early and late phases of the action potential can lead to the development of a variety of arrhythmias, including Brugada, long-QT, and short-QT syndromes as well as catecholaminergic ventricular tachycardia (VT).

Brugada syndrome

The Brugada syndrome is an inherited primary electrical disease in which amplification of TDR is believed to lead to the development of polymorphic VT and sudden cardiac death [52]. The Brugada ECG is characterized by an elevated ST segment or J wave appearing in the right precordial leads (V1–V3), often followed by a negative T wave. First described in 1992, the syndrome is associated with a high incidence of sudden cardiac death secondary to a rapid polymorphic VT or ventricular fibrillation (VF) [53]. The ECG characteristics of the Brugada syndrome are dynamic and often concealed, but can be unmasked by potent sodium channel blockers such as ajmaline, flecainide, procainamide, disopyramide, propafenone, and pilsicainide [54–56].

The Brugada syndrome (BrS) is associated with mutations in *SCN5A*, the gene that encodes the α subunit of the cardiac sodium channel, in approximately 15% of probands [57]. Over one hundred mutations in *SCN5A* have been linked to the syndrome in recent years (see [58] for references; also see http://www.fsm.it/cardmoc). Only a fraction of these mutations have been studied in expression systems and shown to result in loss of function of sodium channel activity. Weiss et al. [59] described a second locus on chromosome 3, close to but distinct from *SCN5A*, linked to the syndrome in a large pedigree in which the syndrome is associated with progressive conduction disease, a low sensitivity to procainamide, and a relatively good prognosis. The

gene was recently identified in a preliminary report as the *Glycerol-3-Phosphate Dehydrogenase 1-Like* (*GPD1L*) gene and the mutation in *GPD1L* was shown to result in a reduction of I_{Na} [60].

The third and fourth genes associated with the Brugada syndrome were recently identified and shown to encode the α1 (*CACNA1C*) and β (*CACNB2b*) subunits of the L-type cardiac calcium channel. Mutations in the α and β subunits of the calcium channel also lead to a shorter than normal QT interval, in some cases creating a new clinical entity consisting of a combined Brugada/short-QT syndrome [61].

Several experimental models of the BrS have been developed using the right coronary-perfused right ventricular wedge preparation [62–66]. The available data point to amplification of heterogeneities intrinsic to the early phases (phase 1-mediated notch) of the action potential of cells residing in different layers of the right ventricular wall of the heart as the basis for the development of extrasystolic activity and polymorphic VT in BrS (Figure 1.3). Rebalancing of the currents active at the end of phase 1 can lead to accentuation of the action potential notch in right ventricular epicardium, which is responsible for the augmented J wave and ST segment elevation associated with the Brugada syndrome (see [52,67] for references). Under physiologic conditions, the ST segment is isoelectric due to the absence of major transmural voltage gradients at the level of the action potential plateau. Accentuation of the right ventricular action potential notch under pathophysiological conditions leads to exaggeration of transmural voltage gradients and thus to accentuation of the J wave or to an elevation of the J point (Figure 1.3). If the epicardial action potential continues to repolarize before that of endocardium, the T wave remains positive, giving rise to a saddleback configuration of the ST segment elevation. Further accentuation of the notch is accompanied by a prolongation of the epicardial action potential causing it to repolarize after endocardium, thus leading to inversion of the T wave [62,63]. Despite the appearance of a typical Brugada ECG, accentuation of the RV epicardial action potential (AP) notch alone does not give rise to an arrhythmogenic substrate. The arrhythmogenic substrate may develop with a further shift in the balance of current leading to loss of the action potential dome at

some epicardial sites but not others. A steep gradient of TDR develops as a consequence, creating a vulnerable window, which when captured by a premature extrasystole can trigger a reentrant arrhythmia. Because loss of the action potential dome in epicardium is generally heterogeneous, epicardial dispersion of repolarization develops as well. Propagation of the action potential dome from sites at which it is maintained to sites at which it is lost causes local reexcitation via phase 2 reentry, leading to the development of a closely coupled extrasystole capable of capturing the vulnerable window across the ventricular wall, thus triggering a circus movement reentry in the form of VT/VF (Figures 1.3 and 1.4) [62,68,69]. The polymorphic VT may start in epicardium reentry, but quickly shifts to an intramural reentry before self-terminating or deteriorating to VF [69].

Evidence in support of these hypotheses derives from experiments involving the arterially perfused right ventricular wedge preparation [62,63,66,69, 70] and from studies in which monophasic action potential (MAP) electrodes were positioned on the epicardial and endocardial surfaces of the right ventricular outflow tract (RVOT) in patients with the Brugada syndrome [71,72].

Long-QT syndrome

The long-QT syndromes (LQTS) are phenotypically and genotypically diverse, but have in common the appearance of a long QT interval in the ECG, an atypical polymorphic VT known as Torsade de Pointes (TdP), and, in many but not all cases, a relatively high risk for sudden cardiac death [73–75]. Ten genotypes of the congenital LQTS have been identified. The identified syndromes are distinguished by mutations in at least eight different ion channel genes, a structural anchoring protein, and a caveolin protein located on chromosomes 3, 4, 6, 7, 11, 17, and 21 (Table 1.1) [76–81].

The most recent genes associated with LQTS are *CAV3* which encodes caveolin-3 and *SCN4B* which encodes $Na_V B4$, an auxiliary subunit of the cardiac sodium channel. Caveolin-3 spans the plasma membrane twice, forming a hairpin structure on the surface, and is the main constituent of caveolae, small invaginations in the plasma membrane. Mutations both in *CAV3* and in *SCNB4* produce a

gain in function in late I_{Na}, causing an LQT3-like phenotype [82,83].

LQTS shows both autosomal recessive and autosomal dominant patterns of inheritance: (1) a rare autosomal recessive disease associated with deafness (Jervell and Lange-Nielsen), caused by two genes that encode for the slowly activating delayed rectifier potassium channel (*KCNQ1* and *KCNE1*); and (2) a much more common autosomal dominant form known as the Romano–Ward syndrome, caused by mutations in 10 different genes (Table 1.1). Eight of the 10 genes encode cardiac ion channels.

Acquired LQTS refers to a QT prolongation caused by exposure to drugs that prolong the duration of the ventricular action potential [84] or QT prolongation secondary to cardiomyopathies including dilated or hypertrophic cardiomyopathy, as well as to abnormal QT prolongation associated with bradycardia or electrolyte imbalance [85–89]. The acquired form of the disease is far more prevalent than the congenital form and in some cases may have a genetic predisposition [90].

Amplification of spatial dispersion of repolarization within the ventricular myocardium has been identified as the principal arrhythmogenic substrate in both acquired and congenital LQTS. The amplification of spatial dispersion of refractoriness can take the form of an increase in transmural, transseptal, or apico-basal dispersion of repolarization. This exaggerated intrinsic heterogeneity together with EAD- and DAD-induced triggered activity, both caused by reduction in net repolarizing current, underlie the substrate and trigger for the development of TdP arrhythmias observed under LQTS conditions [91,92]. Models of the LQT1, LQT2, and LQT3 forms of the LQTS have been developed using the canine arterially perfused left ventricular wedge preparation (Figure 1.5) [93]. These models suggest that in these three forms of LQTS, preferential prolongation of the M cell APD leads to an increase in the QT interval as well as an increase in TDR, which contributes to the development of spontaneous as well as stimulation-induced TdP via an intramural reentry mechanism (Figure 1.6) [35,40,94–97]. The spatial dispersion of repolarization is further exaggerated by sympathetic influences in LQT1 and LQT2, accounting for the great sensitivity of patients with these genotypes to adrenergic stimuli (Figures 1.5 and 1.6).
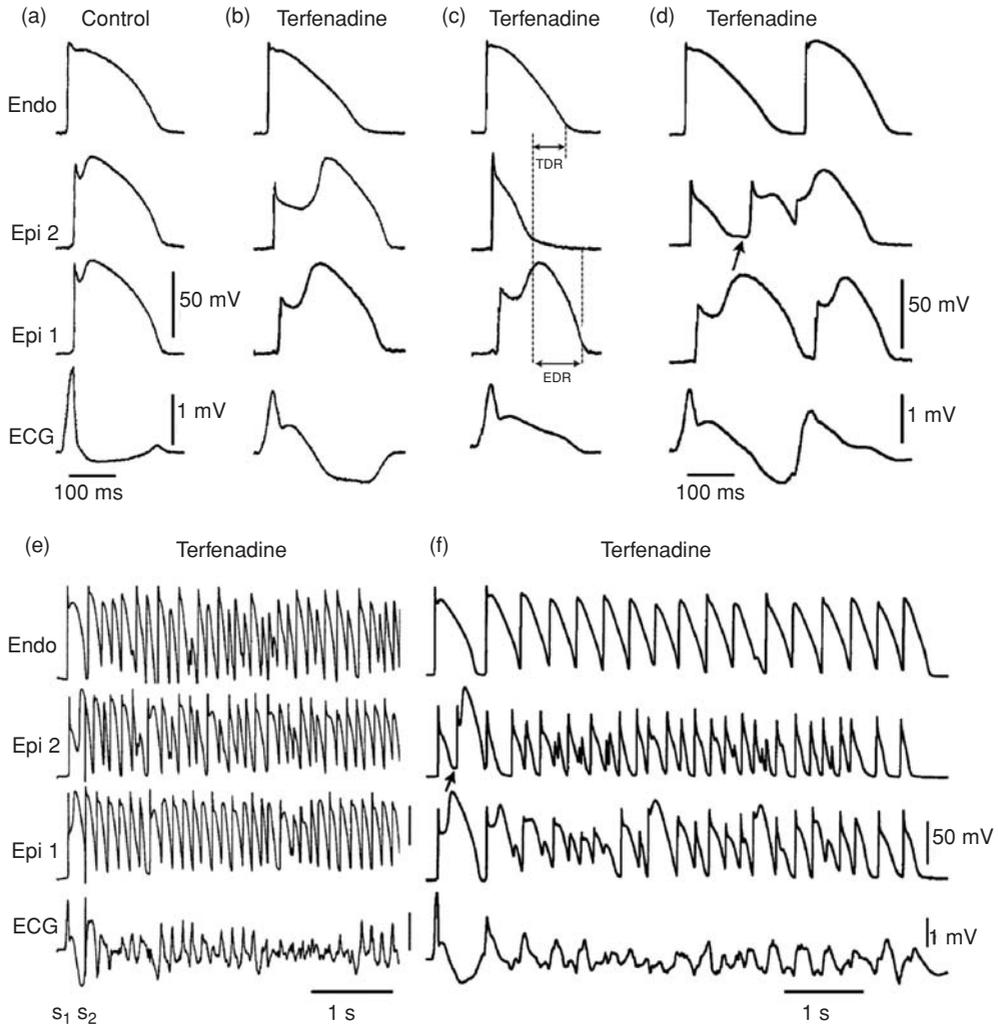
Figure 1.3 Cellular basis for electrocardiographic and arrhythmic manifestation of Brugada syndrome. Each panel shows transmembrane action potentials from one endocardial (top) and two epicardial sites together with a transmural ECG recorded from a canine coronary-perfused right ventricular wedge preparation. (a) Control (BCL 400 ms). (b) Combined sodium and calcium channel block with terfenadine (5 μM) accentuates the epicardial action potential notch, creating a transmural voltage gradient that manifests as an ST segment elevation or exaggerated J wave in the ECG. (c) Continued exposure to terfenadine results in all-or-none repolarization at the end of phase 1 at some epicardial sites but not others, creating a local epicardial dispersion of repolarization (EDR) as well as a transmural dispersion of repolarization (TDR). (d) Phase 2 reentry occurs when the epicardial action potential dome propagates from a site where it is maintained to regions where it has been lost, giving rise to a closely coupled extrasystole. (e) Extrastimulus (S1 – S2 = 250 ms) applied to epicardium triggers a polymorphic VT. (f) Phase 2 reentrant extrasystole triggers a brief episode of polymorphic VT. (Modified from Ref. [63], with permission).

Voltage gradients that develop as a result of the different time course of repolarization of phases 2 and 3 in the three cell types give rise to opposing voltage gradients on either side of the M region, which are in part responsible for the inscription of the T wave [44]. In the case of an upright T wave, the epicardial response is the earliest to repolarize and the M cell action potential is the latest. Full repolarization of the epicardial action potential coincides with the peak of the T wave and repolarization of
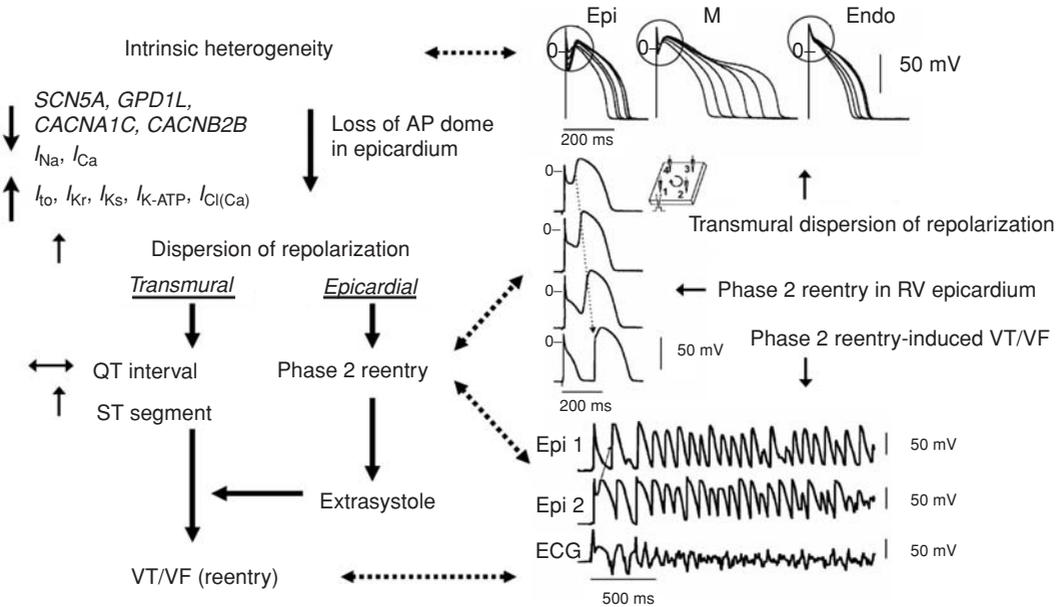
Figure 1.4 Proposed mechanism for the Brugada syndrome. A shift in the balance of currents serves to amplify existing heterogeneities by causing loss of the action potential dome at some epicardial, but not endocardial sites. A vulnerable window develops as a result of the dispersion of repolarization and refractoriness within epicardium as well as across the wall. Epicardial dispersion leads to the development of phase 2 reentry, which provides the extrasystole that captures the vulnerable window and initiates VT/VF via a circus movement reentry mechanism. Modified from [128], with permission.

the M cells is coincident with the end of the T wave. The duration of the M cell action potential therefore determines the QT interval, whereas the duration of the epicardial action potential determines the QT_{peak} interval. The interval between the peak and end of the T wave (T_{peak}–T_{end} interval) in precordial ECG leads is suggested to provide an index of TDR [2]. Recent studies provide guidelines for the estimation of TDR in the case of more complex T waves, including negative, biphasic, and triphasic T waves [98]. In these cases, the interval from the nadir of the first component of the T wave to the end of the T wave provides an approximation of TDR.

Because the precordial leads (V1–V6) are designed to view the electrical field across the ventricular wall, T_{peak}–T_{end} is the most representative of TDR in these leads. T_{peak}–T_{end} intervals measured in the limb leads are unlikely to provide an index of TDR, but may provide a measure of global dispersion within the heart [99,100]. Because TDR can vary dramatically in different regions of the heart, it is inadvisable to average T_{peak}–T_{end} among all or several leads [100]. Because LQTS is principally a left ventricular disorder, TDR is likely to be greatest in the left ventricular wall or septum and thus be best reflected in left precordial leads or V3, respectively [101]. In contrast, because Brugada syndrome is a right ventricular disorder, TDR is greatest in the right ventricular free wall and thus is best reflected in the right precordial leads [102].

T_{peak}–T_{end} interval does not provide an absolute measure of transmural dispersion *in vivo* [100], although changes in this parameter are thought to reflect changes in spatial dispersion of repolarization, including TDR, and thus may be prognostic of arrhythmic risk under a variety of conditions [103–108]. Takenaka et al. [107] recently demonstrated exercise-induced accentuation of the T_{peak}–T_{end} interval in LQT1 patients, but not LQT2. These observations coupled with those of Schwartz et al. [109], demonstrating an association between exercise and risk for TdP in LQT1 but not LQT2 patients, once again point to the potential value of T_{peak}–T_{end} in forecasting risk for the development of TdP. Direct evidence in support of T_{peak}–T_{end} measured in V5 as an index to predict TdP in patients with LQTS was provided by Yamaguchi and co-workers [101]. These authors concluded that T_{peak}–T_{end} is
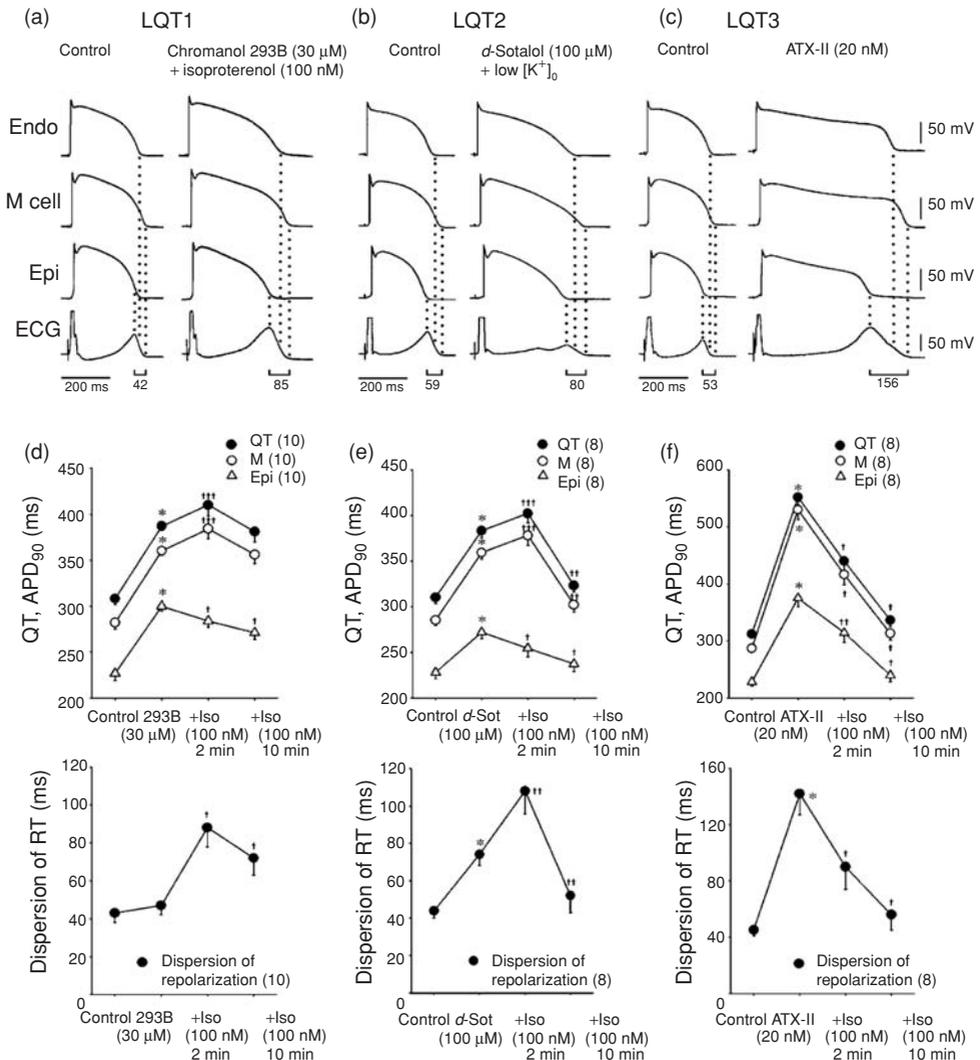
Figure 1.5 LQT1, LQT2, and LQT3 models of LQTS. Panels (a)–(c) show action potentials recorded simultaneously from endocardial (Endo), M, and epicardial (Epi) sites of arterially perfused canine left ventricular wedge preparations together with a transmural ECG. BCL = 2000 milliseconds. Transmural dispersion of repolarization across the ventricular wall, defined as the difference in the repolarization time between M and epicardial cells, is denoted below the ECG traces. LQT1 model was mimicked using Isoproterenol + chromanol 293B — an I_{Ks} blocker. LQT2 was created using the I_{Kr} blocker d-sotalol + low $[K^+]_o$. LQT3 was mimicked using the sea anemone toxin ATX-II to augment late I_{Na}. Panels (d)–(f): Effect of isoproterenol in the LQT1, LQT2, and LQT3 models. In LQT1, isoproterenol (Iso) produces a persistent prolongation both of the APD_{90} of the M cell and of the QT interval (at both 2 and 10 min), whereas the APD_{90} of the epicardial cell is always abbreviated, resulting in a persistent increase in TDR (d). In LQT2, isoproterenol initially prolongs (2 min) and then abbreviates the QT interval and the APD_{90} of the M cell to the control level (10 min), whereas the APD_{90} of epicardial cell is always abbreviated, resulting in a transient increase in TDR (e). In LQT3, isoproterenol produced a persistent abbreviation of the QT interval and the APD_{90} of both M and epicardial cells (at both 2 and 10 min), resulting in a persistent decrease in TDR (f). $*P < 0.0005$ versus Control; $\dagger P < 0.0005$, $\dagger\dagger P < 0.005$, $\dagger\dagger\dagger P < 0.05$, versus 293B, d-Sotalol (d-Sot), or ATX-II. (Modified from references [35,40,94] with permission).